Interactions of Fast μ Mesons in Lead with Small-Energy Transfer*†

J. DE PAGTER‡ AND R. D. SARD
Department of Physics, Washington University, St. Louis, Missouri
(Received September 25, 1959)

With the Pb target material divided into 1.27-cm slabs between hodoscoped Geiger tubes and surmounted by a magnet cloud chamber, a study has been made of the interactions of fast μ mesons in which at least one evaporation neutron is produced and no additional charged particles emerge from the slab. The cross section-average neutron multiplicity, $\sigma\bar{m}$, is $(15.2\pm2.1)\times10^{-29}$ cm^2 per nucleon. From hodoscope observations without neutron coincidence it is found that for an electron-initiated shower to stay concealed in a 1.27-cm Pb plate its energy must be less than about 100 Mev. With the help of "approximation B" track length theory and experimental photonuclear neutron yields, we calculate that hidden knock-on showers contribute $(5.8\pm1.2)\times10^{-29}$ to the total yield $\sigma\bar{m}$ (cross section times average multiplicity), leaving $(9.4\pm2.4)\times10^{-29}$ cm^2 per nucleon as the result for the direct μ-meson nuclear interaction. This analysis is supported by the agreement between the number of visible showers observed and calculated. The neutron yield in the direct interaction is found to increase with μ-meson momentum. The Weizsäcker-Williams approximation is used to calculate the effect expected from the interaction between the electric charge of the μ meson and the nucleons. Within the rather large uncertainties involved in the use of this approximation, there is excellent agreement with the experimental results.

I. INTRODUCTION

SINCE the discovery of the production of evaporation neutrons by fast μ mesons,[1] that phenomenon has been the subject of several experiments at this laboratory.[2] The study of the direct μ-meson-nucleus interaction is complicated by the presence of two other mechanisms giving rise to the detection of an evaporation neutron associated with the passage of a penetrating cosmic-ray particle. One is the direct nuclear interaction of fast protons. Though fast protons only constitute some 0.9% contamination of the sea-level cosmic ray μ-meson beam, their cross section for nuclear interaction is much greater than that of the μ mesons, so that they could contribute appreciably to the observed neutron yield. The other mechanism is production of an energetic knock-on electron by a μ meson, a photon in the resulting cascade shower giving rise to a photonuclear neutron. The present experiment embodies features which should permit clear separation of these effects from the direct μ-meson-nucleus interaction. It is also designed to show the dependence of the μ-meson-nucleus interaction on μ-meson energy in the Bev range.

II. APPARATUS

The geometrical arrangement is shown in Fig. 1. As in the experiment of Stearns et al.,[2] the Pb target material and its surrounding neutron detecting array are located under the Washington University magnet cloud chamber. The chamber is triggered by an event designated $(ABC:N)$—an (ABC) prompt coincidence followed by the detection in the $B^{10}F_3$ proportional counters of at least one thermalized neutron in delayed coincidence (5–230 μsec). A filter of 22.9 cm Fe is placed between the target material embraced in the neutron detector and the C tray. The target material—Pb alloyed with 4% Sb—is divided into six $\frac{1}{2}$-inch slabs and one 3-inch one, with Geiger tubes above, below, and in between connected to form a hodoscope [i.e., when an $(ABC:N)$ event occurs, a record is made for each Geiger tube as to whether or not it discharged in prompt coincidence with (ABC)]. The electronic circuits also provide a record of the number of neutrons detected in the delayed coincidence gate.

Discrimination against proton interactions is provided by the determination of the sign of the charge of the entering particle by means of the magnet cloud chamber, by the observation of possible shower development in the multiple-layer hodoscope, and by the requirement of penetration through the 22.9 cm Fe filter between the target and the C tray. Proton interactions are known to be quite catastrophic; according to the observations of Mylroi and Wilson[3] at sea level, in at most 10% of the proton interactions does a particle capable of penetrating 5–10 cm Pb emerge. If a proton interaction does give a penetrating secondary, it would make a shower in the hodoscope. So, if the data are restricted to interactions by penetrating particles showing no multiplicity in the hodoscope, the proton contribution to it should be small. Finally, the sign of the

* Based on the thesis submitted by J. de Pagter to Washington University, April, 1958, in partial fulfillment of the requirements for the degree of Doctor of Philosophy. Some of the results were presented at the New York meeting of the American Physical Society, January, 1958 [J. de Pagter and R. D. Sard, Bull. Am. Phys. Soc. 3, 34 (1958)].

† Supported by the joint program of the Office of Naval Research and the U. S. Atomic Energy Commission.

‡ Now at the Cambridge Electron Accelerator, Harvard University, Cambridge, Massachusetts.

[1] R. D. Sard, Phys. Rev. **80**, 134(A) (1950); R. D. Sard, M. F. Crouch, D. R. Jones, A. M. Conforto, and B. F. Stearns, Nuovo cimento **3**, 326 (1951).

[2] H. C. Wilkins, Ph.D. thesis, Washington University, September, 1952 (unpublished); M. Annis, H. C. Wilkins, and J. D. Miller, Phys. Rev. **94**, 1038 (1954); E. J. Althaus and R. D. Sard, Phys. Rev. **91**, 373 (1953); B. F. Stearns, D. R. Jones, J. de Pagter, and R. D. Sard, Phys. Rev. **106**, 1043 (1957).

[3] M. G. Mylroi and J. G. Wilson, Proc. Phys. Soc. (London) **A64**, 404 (1951).

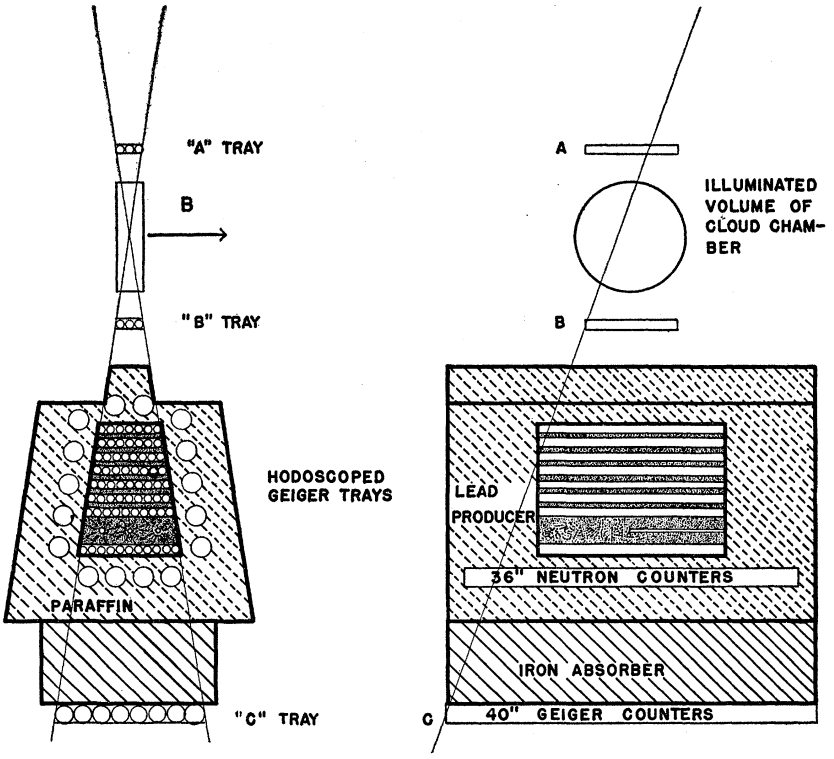

FIG. 1. Geometrical arrangement. The magnet cloud chamber is between the A and B trays of the Geiger tube telescope ABC. The Pb target material forms a "sandwich" with eight layers of hodoscoped Geiger tubes. It is enclosed in a paraffin wax $B^{10}F_3$ proportional counter neutron detecting system.

entering particle provides a check, as the number of negative protons at sea level is negligible. Protonic contamination would make the ratio of positive to negative particles larger than the well-known value for sea level cosmic ray μ mesons.[4]

There is very little dense material above the target, in order to minimize effects due to secondaries of local interactions. To be accepted in the analysis, the cloud chamber picture is required to show one and only one counter age track.

The main reason for dividing the target material into thin slabs with hodoscoped Geiger tubes in between is to detect knock-on electron showers. The arrangement is an approximation to a multiplate cloud chamber for observation of shower development. The procedure for estimating the number of hidden knock-on showers from the number actually seen will be discussed in detail below.

The Pb target material was alloyed with Sb to give the necessary strength to the slabs to permit mounting them by the edges. A test showed that the Sb content has no effect on the neutron detecting efficiency. The target material is enclosed by the neutron detecting array, an 8-inch thick shell of paraffin in which are the sixteen BF_3 counters,[5] of 2-inch diameter by 38-inch active length, at a depth of 2 inches from the inside surface. The 4 inches of paraffin left behind the counters reduces the sensitivity to neutrons from outside. The measured efficiency in detecting neutrons from a calibrated Ra-Be source placed in the target is 12.1%, and uniform throughout the target material to within 5% of that figure. The large efficiency for this type of detecting system is due no doubt to the almost complete enclosure of the target by the long counters, the solid angle subtended by the detector exceeding 2π steradians for every point of the target. The efficiency for detection of coherent neutrons in the 225 μsec coincidence gate is reduced, because of the 150 μsec mean life in the detector, to 9.3%. This value is considered to be correct within $\pm 10\%$, the uncertainty in the absolute calibration of the source.

The cloud chamber[6] is a 13.5-inch internal diameter glass cylinder closed at the back by a 12-inch diameter magnesium piston mounted on a Neoprene diaphragm and at the front by a glass-water-glass double window. The region illuminated and photographed is 12 inches in diameter by 3 inches deep. The chamber is filled with argon and vapor from 63:37 ethanol-water mixture to a total pressure of 96 cm Hg at 27°C.

The expansion ratio is controlled by the position of the piston when the chamber is compressed, which is

[4] G. Puppi in *Progress in Cosmic Ray Physics* (North-Holland Publishing Company, Amsterdam, 1956), Vol. III, p. 365.

[5] The counters were made by the N. Wood Counter Laboratory, Chicago, Illinois, using enriched boron provided by the Isotopes Division of the U. S. Atomic Energy Commission.

[6] A more detailed description of the cloud chamber and electromagnet can be found in B. F. Stearns' Ph.D. Thesis, Washington University, September, 1956 (unpublished). The design and construction of the magnet cloud chamber system was a group effort, but particular credit should be given to D. R. Jones for his contribution to the basic design.

in turn controlled by the pressure applied behind the piston. The motion of the piston from the forward position to the back stop takes place in 6 msec, without bouncing. The track width is about 0.7 mm in the chamber. The delay before flashing the lights is 50 msec. To minimize convection currents, pre-existing or arising during this period, an elaborate thermal jacketing system is used. Water is pumped around the chamber at the rate of 30 gallons per minute through passages in thermal contact with every metal portion of the chamber frame and also with the water cell in the double front window. As the magnet yokes run at a higher temperature than the chamber, the water is made to run from bottom to top, warming with heat absorbed from the magnet yoke as it goes. The gradient obtained in this way is 0.1°C. The input temperature of the water is controlled to within 0.01°C. The room temperature is kept 2–4°C below that of the jacket by means of an air conditioner. Under these conditions the chamber is free from convection currents. At the same time, there is no indication of nonuniformity of condensation. A sample picture, showing an unaccompanied positive particle of 15 Bev/c, is reproduced in Fig. 2. The figure also shows the hodoscope record of a particle penetrating the target without making a visible secondary and without appreciable scattering (no effort was made to locate the neon lamps exactly to scale).

The magnetic field is 8500 gauss at the center of the chamber. The extreme variations of the axial field in the illuminated region are $+14.6\%$ and -12.2%. The actual variations along a track selected by our telescope are a good deal smaller because of the limited dip (6°) and slant (18°) that are permitted. In any event, the calculation of the momentum from the measured curvatures on the film makes use of the measured field distribution, so that the inhomogeneity is only of computational concern. The coils of the magnet are wired in two groups, which can be connected either in conjunction (usual operating condition) or in opposition ("zero-field" runs) without alteration of the heat production in the copper. Zero-field runs were interspersed throughout the period of taking data, in order to determine the precision of the momentum measurements.

III. TECHNIQUE OF MOMENTUM MEASUREMENT

The curvatures of the track images were measured on a prism compensator.[7] In this instrument one balances out the track curvature by introducing a variable curvature of opposite sign. This null method is fast, and more than accurate enough for our purpose, as shown by the zero-field curvature distributions presented below.

[7] P. M. S. Blackett, Proc. Roy. Soc. (London) **A159**, 1 (1937). A careful study of the errors has been made by K. H. Barker (Thesis, Manchester, 1952). Details of our instrument, procedure, and calibration can be found in J. de Pagter, Thesis, Washington University, April, 1958.

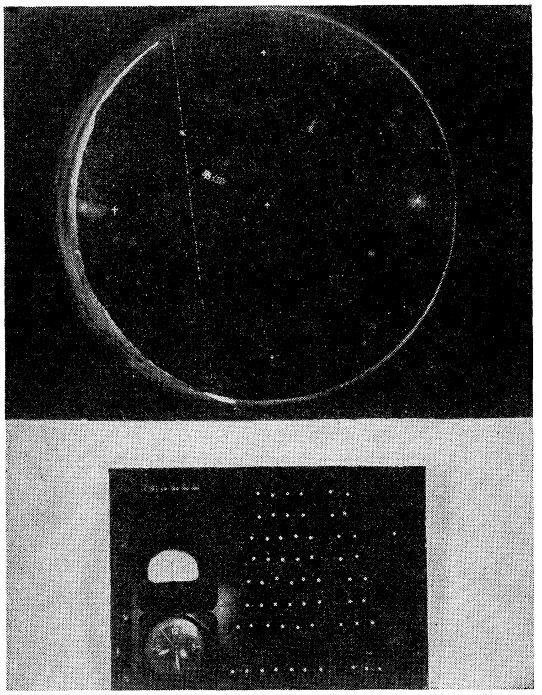

FIG. 2. Sample cloud chamber and hodoscope picture. The cloud chamber picture shows a single positively charged particle of 15 Bev/c momentum. The hodoscope picture shows that it penetrated the target hodoscope without any extra Geiger tubes being discharged and without appreciable scattering (the neon lights are not positioned exactly to scale).

In order to calculate the momentum from these measurements, one must determine the position of the track in the chamber. This has been found by reprojecting the pair of views back through the same lenses which were used to take the picture onto a movable screen perpendicular to the axis of the projector. The coordinates of a blob are found by moving the screen in and out along the axis until the two images of the blob coincide. The depth coordinate must, of course, be corrected for the effects of the window, which is absent from the re-projection arrangement, and of the gas expansion. The former is eliminated by measuring depth relative to that of the reprojected image of the velvet on the piston. The latter is calculated on the assumption of a uniform strain equal to the expansion ratio minus one.

The effective magnetic field was taken to be the value of the axial field at the center of the track. This assumption should not introduce an error of more than 2 or 3%.

Correction must be made for the curvature introduced by the camera lenses and the chamber window. The correction for this systematic error was determined by photographing a set of fine wires under tension mounted in the chamber, measuring the coordinates of the wire images by means of a Gaertner comparator and computing the curvature of the image by a least-squares

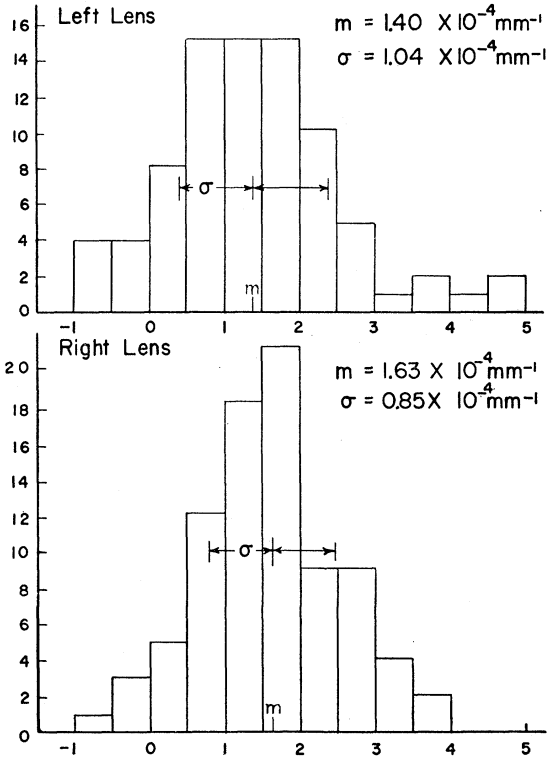

FIG. 3. Histograms of the corrected curvature in image space, for the two lenses, of 82 zero field tracks. The curvature is in units of 10^{-4} mm^{-1} on the film, corresponding to an inverse momentum for a track in the middle of the chamber of (29.3 Mev/c)$^{-1}$. By each histogram is written the mean and the standard deviation.

procedure.[8] For each lens curves were then plotted of distortion curvature as a function of position, and the appropriate ordinate was subtracted from the measured track curvature. Unfortunately the wires were photographed at $f/8$ while the cloud tracks were photographed at $f/11$. As the lenses (selected Zeiss Biotars, 40 mm focal length, $f/2$) are very much stopped down, there should be little change in the distortion between $f/8$ and $f/11$.

With the small dip and slant angles of our tracks, the corrections for conical projection and radial magnetic field amount to less than 1%,[6] and may be neglected.

Information on the over-all precision of momentum measurement is given by the histogram of the no-field curvatures. The results for some 82 tracks are shown in Fig. 3, the data for the two lenses being plotted separately. The agreement in mean and standard deviation indicates that the optical corrections (which are very different for the two lenses, and considerably larger than the widths of the histograms) are accurate, for the two lenses are, after all, making images of the same tracks. The displacement of the mean from zero curvature, by 1.5×10^{-4} mm^{-1} on the film, corresponding to 20 Bev/c, shows that there is a residual systematic error.[9] Correction is made for this error, as well as the optical one, in calculating the momentum. The widths of the histograms imply a remarkably small random error, the standard deviations being 1.04×10^{-4} mm^{-1} and 0.85×10^{-4} mm^{-1} for the left and right lenses, respectively, corresponding to 28 and 35 Bev/c.

The momentum is, then, calculated from the curvature on the film, corrected for systematic errors; the axial magnetic field at the center of the track; and the magnification appropriate to the depth in the chamber of the center of the track. That the over-all correction for systematic errors is accurate is shown by the reasonable shapes of the momentum spectrums of interacting positive and negative particles presented below (Fig. 4). A small residual systematic error would result in a large excess of particles of one sign in the middle of the spectrum. To allow for residual uncertainties in the systematic corrections, we take as our "maximum detectable momentum"[10] 20 Bev/c; i.e., a

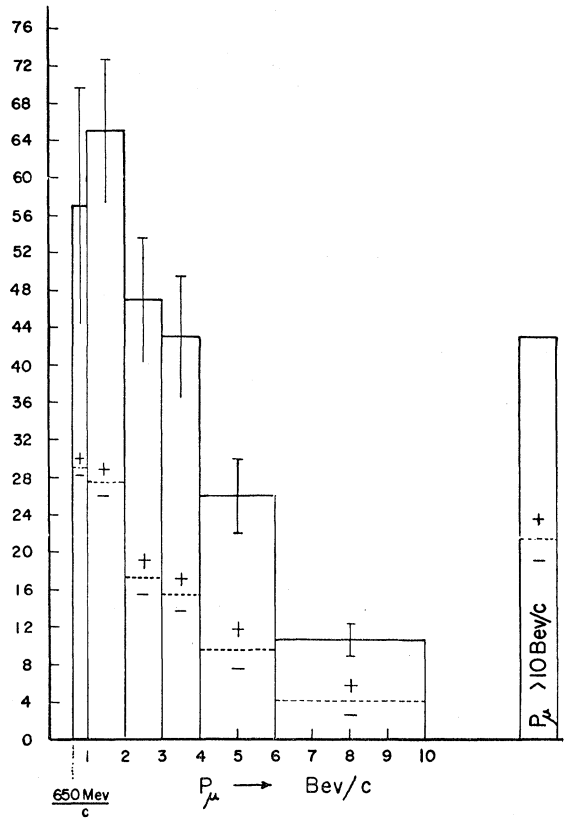

FIG. 4. Histogram of the momentum of a set of 311 Type I $ABC{:}N$ tracks, selected on the basis of length in the chamber.

[8] J. E. Rizzo, Jr., M.A. Thesis, Washington University, January, 1959.

[9] The cause of this systematic error is not known. A similar residual shift of the no-field histogram has been reported by R. W. Thompson [*Progress in Cosmic-Ray Physics* (North Holland Publishing Company, Amsterdam, 1956), Vol. III, p. 253, Fig. 2], who used a more objective method of measuring curvature.

[10] P. M. S. Blackett and R. B. Brode [Proc. Roy. Soc. (London) **A154**, 573 (1936)] and, following them, R. W. Thompson [*Progress*

TABLE I. Data and corrections. The total number of $(ABC:N)$ events is 541, of (ABC) 532. The categories Type I, Type II, and Type III are defined in the text.

	Type I (no shower or knock-on)		Type II (knock-on)		Type III (shower)	
	(ABC)	$(ABC:N)$	(ABC)	$(ABC:N)$	(ABC)	$(ABC:N)$
1. Raw data	442	358	47	85	9	98
2. Normalized to $\frac{1}{2}$-inch slabs	405±23	305±20	74±11	111±14	19±6	125±14
3. Correction for accidental coincidences		−(144±3)		−(26±1)		−(7±2)
4. Correction for unassociated type II and III events		+(95±15)		−(75±11)		−(19±6)
5. Corrected number of events		262±25		10±18		99±15

momentum of p Bev/c has an estimated standard error of $p^2/20$ Bev/c.

IV. DATA

During a total sensitive time of 44 055 minutes, 541 cloud-chamber and hodoscope pictures were taken using the $ABC:N$ trigger which fitted the following specifications.

1. There was a single, minimum-ionization track in the cloud-chamber.

2. Only one Geiger tube was discharged in the hodoscoped Geiger tube tray above the first lead plate.

3. The particle, as shown in the hodoscope picture, did not appear to stop. (The geometry of the experiment was such that it was possible for a particle to miss part of the hodoscope and still be in the solid angle of the ABC telescope. Discarding these merely makes the bottom tray of the hodoscope partly determine the solid angle of the apparatus.)

A run was also made in which no detected neutron was required (ABC alone) to enable the background corrections to be determined. A total of 532 ABC pictures were taken which met the above specifications.

Both the $ABC:N$ and ABC data were grouped into three categories, as shown in Table I. Type I are cases in which the particle penetrated the entire hodoscope without giving rise to any detected showers in the hodoscope. (A detected shower is defined here as an event in the hodoscope in which one or more counters were discharged which were not in the direct line of flight of the particle.) Type II are identical to Type I except that in some one hodoscope tray two adjacent counters were discharged; presumably these are due to a lone knock-on electron, or a small knock-on shower. Type III events are the remaining detected showers.

Interactions by μ mesons in which there is a large energy transfer would in all likelihood produce visible multiplicity in the hodoscope and be therefore experimentally indistinguishable from neutron producing knock-on showers. This has led to an attempt to find separately the number of neutrons produced by μ mesons in interactions where the energy transfer is small, corresponding to there being no visible secondary under a 1.27 cm ($\frac{1}{2}$ inch) Pb plate. To this end the following corrections to the number of Type I events must be made.

The first correction, embodied in the second row of Table I, is to estimate the number of Type I, II, and III events which would have been seen had all rather than only half of the producer been divided into half-inch slabs. For the Type III events there were 22 of the 98 seen which would have appeared as Type I if the first three inches of lead had been solid. Similarly 31 of the 85 Type II events would then have been classed as Type I. There were also 5 Type III events which had been initiated in the second tray and which were contained in the first three inches of lead. This last number is used to estimate the number of Type III events which were classed as Type II because they started in the slab just above the three inch thick block. These two types of events are not exactly equivalent to each other, for the latter had an extra half-inch of lead in which to develop, but since this correction is small in the first place the error is very minor. The total number of Type III events which would therefore have been identified, had the bottom three inches of lead been divided into half-inch slabs, is $98+22+5=125$. Similarly, there would have been $85+31-5=111$ Type II events and only $358-22-31=305$ Type I events.

In the same way, in the ABC run there were 8 Type III and 29 Type II events which would have appeared as Type I had the upper three inches of the lead producer block been undivided, and 2 cases of Type III which would have appeared as Type II had they started in the seventh tray. Therefore the corrected numbers of ABC events are 405 Type I, 74 Type II, and 19 Type III.

The errors tabulated are statistical. They have been calculated by squaring the errors of the component terms, adding, and taking the square root. Due care must be used that the components chosen are statistically independent. For each one the standard error is estimated as the square root of the number of events.

The third row of the table gives the correction for accidental coincidences between the penetration of the hodoscope and the A, B, and C trays by a charged particle and the detection of an unassociated neutron

in Cosmic Ray Physics (North Holland Publishing Company, Amsterdam, 1956), Vol. III, p. 253] specify the precision by the probable error of the Gaussian fitted to the no-field histogram. On this basis, our "maximum detectable momentum" is 30 Bev/c.

by the neutron counter array. It is determined as in the following example. The background correction to the 305 Type I $ABC:N$ events is the product of the ABC rate, the $ABC:N$ running time, the fraction of ABC events that are of Type I, the $ABC:N$ coincidence gate length, and the background neutron counting rate:

$$C_{Bg}(\text{Type I})=(4.30/\text{min})\times 44\,055\ \text{min}\times(405/532)\times 225\times 10^{-6}\ \text{sec}\times 4.438/\text{sec}=144.$$

Since all of these quantities are very well known relative to the statistical errors in the data, with the exception of the fraction of ABC events of Type I, 405/532, the error in the expected background contribution is almost entirely due to the error in that ratio. The fractional error in the ratio was calculated in the same manner as before and is 2.32×10^{-2}, so the error in the 144 is $144\times 2.32\times 10^{-2}=3.3$. The background contributions and errors for Type II and III events are calculated in a similar manner, and all are to be found in Row 3 of Table I.

The final correction (Row 4) is for true Type I events in which the μ meson also produces an unrelated knock-on or shower visible in the hodoscope, leading to classification as Type II or III. This number can be computed if it is assumed that the probability of a μ meson producing a visible knock-on or shower is essentially the same in the ABC and $ABC:N$ runs. This is not strictly true, for the spectrum of μ mesons in the cosmic radiation would be expected to be different from the spectrum of μ mesons interacting with nuclei, as the interaction probability is dependent on energy. However, the difference is not important in this case. The correction is taken from the (ABC) data, and for the Type I events is simply the fraction of Type II and Type III events found in the (ABC) run times the total number of (ABC) events:

$$[(74+19)/532]\times 541=95\pm 15$$

the error being calculated as before.

The fifth row shows the final corrected totals normalized to $\frac{1}{2}$-inch Pb slabs. For the Type I events the number is 262 ± 25, confirming clearly the existence of low-energy transfer interactions of fast μ mesons.[1] For the Type II events (small showers), it is seen that there is no evidence for any neutron production in this type of event—suggesting that showers concealed in the $\frac{1}{2}$ inch plates make only a small contribution to the Type I yield. The result for Type III events—99 ± 15—shows unequivocally the production of evaporation neutrons in association with sizeable showers.

The number of Type I events, 262 ± 25, translated into a cross section-neutron multiplicity product per μ meson is $(15.2\pm 1.5)\times 10^{-29}$ cm^2 per nucleon in Pb. There is an additional 10% error in the absolute neutron detecting efficiency. The number of Type III events 99 ± 15, corresponds to $(5.8\pm 0.9)\times 10^{-29}$ cm^2 per nucleon. The total neutron yield from the direct and shower effects is $15.2+5.8=(21\pm 2.7)\times 10^{-29}$ cm^2 per nucleon.

The experiment also gives the momentum spectrum of the interacting μ mesons. In Fig. 4 is shown a histogram of the number of tracks per Bev/c momentum interval of Type I $ABC:N$ events. It contains 311 tracks selected on the basis of length in the cloud chamber. The momentum interval increases with momentum to keep step with the increasing uncertainty in the momentum measurement ($p_{\max}=20$ Bev/c). The numbers of positive and negative particles in each momentum interval are shown. The positive-negative ratio is 1.50 ± 0.18, as compared to the known value for μ mesons of 1.25. This difference is not outside the bounds of a reasonable statistical fluctuation. Since the Fe filter should discriminate strongly against proton interactions which are not recognized in the hodoscope, it is felt that the difference does not represent a proton contamination. In any event a proton contamination of the order of 10% would have little effect on the results.

The approximate constancy of the positive:negative ratio in the histogram shows that proper allowance for systematic errors in the curvature measurements has been made. Otherwise there would be a pronounced bump or dip in the ratio, the spectra of positives and negatives being shifted in opposite directions.

The experimental spectrum of apparent Type I ($ABC:N$) events contains, in addition to direct nuclear interactions, accidental coincidences and concealed knock-on showers. The background correction has the spectral shape of the incident radiation. Its area equals the ABC rate$\times$running time$\times F\times F'\times ABC:N$ gate length$\times N$ rate$=107\pm 7.5$. Here F is the fraction of ABC pictures that appear to be of Type I and F' is the fraction of $ABC:N$ Type I pictures selected for momentum measurement. The error results mainly from the uncertainties in $F\times F'$. The shape of the correction is not, however, subject to any such uncertainty, for the spectrum of sea-level μ mesons[11] is known accurately in the momentum range under consideration.

The knock-on shower correction is obtained from the numerical calculation outlined in Sec. V, and we defer discussion of it until Sec. VI. The area comes out to be 63 ± 13 events. The shape of the curve is much less in doubt than its height. The final Type I $ABC:N$ μ-meson momentum histogram corrected for background and knock-on showers, i.e., referring to direct μ-meson-nuclear interactions, is shown in Fig. 5. The first graph (a) is our best estimate. In (b) and (c) the knock-on shower correction is respectively lowered and raised by an amount corresponding to 13 events. (The smooth curve is the theoretical prediction worked out in Sec. VI, adjusted in height to fit each experimental histogram.)

[11] B. G. Owen and J. G. Wilson, Proc. Phys. Soc. (London) **A68**, 409 (1955).

By comparing the shape of the experimental momentum spectrum of interacting μ mesons with that of the incident μ mesons, we can find the dependence on momentum of the cross section-neutron multiplicity product. For three ranges—0.65 to 3 Bev/c, 3 to 10 Bev/c, and 10 Bev/c on up—the ratio has been computed of the number of detected interactions to the fractional area under the incident μ-meson spectrum. The results, using the histogram of Fig. 5(a), are shown in the first row of Table IV, normalized to unity for the first interval. The errors indicated are only statistical. Even allowing for the additional errors in the corrections there is still a significant rise in the neutron yield with μ-meson momentum.

V. CONTRIBUTION TO THE COUNTING RATE BY KNOCK-ON SHOWERS

In order to determine the true number of direct μ-meson nuclear interactions in the Type I category we need to find out what fraction of the detected neutrons associated with these events are the result of photonuclear absorption of real photons in small knock-on showers hidden in the producer slabs. To this end a calculation of the contribution to the $ABC{:}N$ counting rate by knock-on showers has been made using the "approximation B" shower theory[12] and the Jones and Terwilliger measurements[13] of the photonuclear neutron yield in lead.

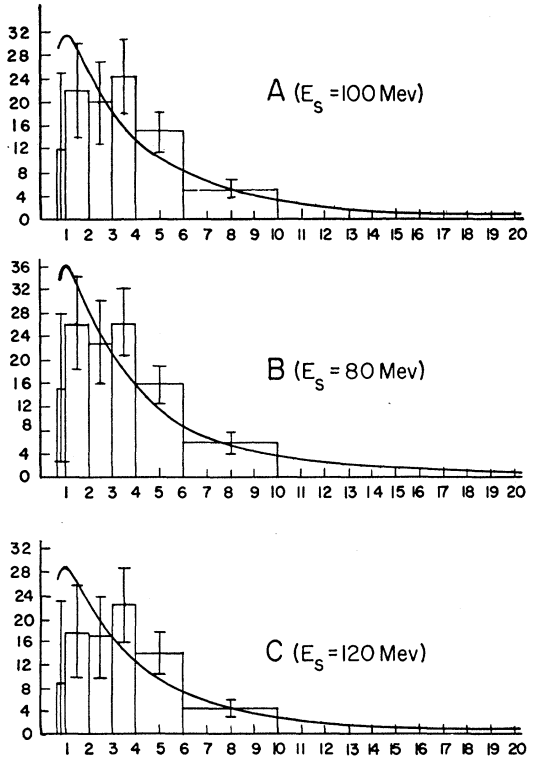

FIG. 5. Momentum histogram of nuclear-interacting μ mesons, corrected for background and concealed knock-on showers. (a) Best estimate; (b) knock-on correction larger by one estimated standard deviation; (c) knock-on correction smaller by one estimated standard deviation.

The number of neutrons from knock-on showers per incident μ meson, Y_{k0}, can be written[14] as a triple integral over photon energies, knock-on electron energies capable of giving the photon energy in question, and μ-meson momenta capable of giving the particular knock-on electron energy. The integrand contains the photonuclear neutron yield (i.e., cross section times average neutron multiplicity) as a function of photon energy, the photon "track length"[12] per unit energy interval in the shower, the cross section for producing a knock-on electron per unit knock-on energy interval, and the differential momentum spectrum of the incident μ mesons.

To facilitate the integration over the photon energy, simple approximations of the Jones and Terwilliger data,[13] were used. The giant resonance peak at 15 Mev was represented by a delta function. In view of the slow variation of photon track length with energy this is an excellent approximation. The slow rise between 20 and 320 Mev fitted quite closely a linear function. For energies above 320 Mev, no data for complex nuclei are available. It is expected that the cross section will decrease with increasing energy while the neutron multiplicity will, of course, increase. We have therefore assumed that the yield, $\sigma\bar{m}$, remains constant at its value at 320 Mev. In any case, the contribution to the counting rate by high-energy photons turns out to be small, and in cases where the shower is undetected by the hodoscope (Type I events) the contribution should be essentially nil. The expressions used are the following:

(1) $\sigma\bar{m}(\mathrm{GR})=\delta(E_\gamma-15\ \mathrm{Mev})\times 5.1\times 10^{-24}\ \mathrm{cm^2/atom}$

(2) $\sigma\bar{m}(20<E_\gamma<320)=2\times 10^{-27}\ \mathrm{cm^2/atom}\times E_\gamma$

(3) $\sigma\bar{m}(E_\gamma>320\ \mathrm{Mev})=6.4\times 10^{-24}\ \mathrm{cm^2/atom}.$

For the differential photon track length the approximation B expression as given by Rossi and Greisen.[15] was used, corrected for the energy dependence of the pair production cross section by multiplication by the ratio of the asymptotic value for large energy to that at the energy in question.[16] The expression used for the differential knock-on cross section was the Bhabha spin-$\frac{1}{2}$ formula.[17]

The μ-meson spectrum was that measured by Owen and Wilson[11] up to 20 Bev/c, extrapolated to higher energies by the analytic expression given by them. The

[12] See, for example, B. Rossi, *High Energy Particles* (Prentice-Hall, Inc., Englewood Cliffs, New Jersey, 1952), Chap. 5.

[13] L. W. Jones and K. M. Terwilliger, Phys. Rev. **91**, 699 (1953).

[14] The details can be found in Chap. 5 of the thesis on which this article is based: J. de Pagter, Thesis, Washington University, St. Louis, April, 1958.

[15] B. Rossi and K. Greisen, Revs. Modern Phys. **13**, 240 (1941), Eqs. (2.96), (2.87), and Fig. 18.

[16] As in Eq. (5 19 9) of reference 12.

[17] H. J. Bhabha, Proc. Roy. Soc. (London) **A164**, 257 (1938).

smallest momentum considered is 0.65 Bev/c, corresponding to the range required for an ABC event.

The result of the integration is

$$Y_{k0}=8.04\times10^{-4}z,$$

where z is the thickness of Pb in cm; this corresponds to a cross section-neutron multiplicity product of 11.8×10^{-29} cm^2 per nucleon in lead. A calculation considering only the giant resonance part of the photonuclear cross section gives $7.12\times10^{-4}z$, which is 88% of the total yield. The assumed constant portion of the photonuclear cross section, above 320 Mev, contributes less than 4%.

The number of events of Type I, II, and III which were initiated by knock-on showers is obtained by multiplying Y_{k0} by the ABC rate, the running time, the fraction of ABC events produced by penetrating μ mesons, and the coherent neutron detection efficiency.

$$N_{k0}=8.04\times10^{-4}\times(15.3\times4.30/\text{min})\times44055\text{ min}\times(498/532)\times0.093=203.$$

The errors in this number arise principally from the uncertainty in the photon track length in the region of the giant resonance, which contributes almost all of Y_{k0}. The uncertainty in the giant resonance contribution results from the fact that the shower theory track length expression involves the assumption that the photon energy is large compared to the critical energy for the substance. In choosing a material of large atomic number like lead this error was minimized, the giant resonance energy for lead being twice the critical energy. In iron, on the other hand, the two are roughly equal. The uncertainties in the μ-meson spectrum and in the knock-on probability are small compared to the statistical uncertainties in this experiment. The problem of estimating the error in the track length formula at the giant resonance energy is, however, a very difficult one. There is no direct experimental evidence on this question, and so it can only be approached by comparing calculations which have utilized different means and different approximations.

The effect of the principal simplifications made in approximation B shower theory, namely that the Compton effect may be neglected and that electrons undergo a continuous collision energy loss in penetrating matter which is independent of the electron energy, can be appreciated in a comparison made by Rossi[18] in the special case of a very high initiating energy for the shower. This comparison is between a numerical calculation of the differential electron track length in air by Richards and Nordheim[19] in which account is taken of the Compton effect and collision processes are considered in detail, and a similar calculation by Tamm and Belenky[20] which used approximation B. At twice the critical energy the difference is some 4% and has only risen to around 12% at the critical energy. On the other hand, Wilson's[21] Monte Carlo calculations for the number of electrons of any energy as a function of depth for showers of less than 300 Mev give a markedly different result from the approximation B shower theory. For example, the peak value for 100-Mev showers is only 60% as high, but the shower penetrates further than in shower theory. This characteristic persists at the other energies studied. The track length should not, however, be much less, as it is obtained by integrating over the whole development of the shower. Our result, $N_{k0}=203$, is somewhat but not much over-estimated.

We have now to estimate what fraction of these events are of a size to be hidden in a single plate, so as to be included in the Type I events. Our approach is the same as that of Annis and Wilkins.[2] It is first recognized that the detection efficiency of the hodoscope for showers is very small for low-energy showers and approaches one for large showers. A not unreasonable first approximation, then, is that it is zero for all showers below a certain energy (E_s) and one for all showers above that energy. This cutoff energy can be estimated from the data.

It is expected that almost all of the Type III ABC events are large knock-on showers. The possibility that they are proton interactions is quite remote—as pointed out in the introduction, the frequency of protons is about 0.9% of the μ-meson flux at sea level and the requirement that the secondary products of the interaction penetrate nine inches of iron should reduce the probability of proton contamination to a very small figure. It is also very unlikely that there would be low-energy knock-on electrons accompanying the meson out of two adjacent plates. If all the knock-on electrons were to be detected, and this is an unrealistically high estimate, this probability would be[22] of the order of $(7\times10^{-2})^2$. An upper limit for E_s can therefore be obtained by comparing the percentage of Type III events in the ABC run with the curve giving the probability for sea level μ mesons of making a knock-on electron of energy exceeding E_s as a function of E_s. This curve was calculated from the knock-on probability, which is a function of the electron energy and the μ-meson energy, and the sea level μ-meson spectrum. Type III showers were detected in 3.8 ± 1% of the ABC events which fitted into one of the three categories. We read off from the curve that this range of frequencies corresponds to a cutoff energy E_s of 107_{-18}^{+27} Mev.

It is clear that the cutoff for detecting Type II showers should be at a lower energy than this, although how much lower is not certain. According to Wilson's[21] Monte Carlo calculations, the probability of finding one or more electrons after two radiation lengths is

[18] See reference 12, pp. 278–282.
[19] J. A. Richards and L. W. Nordheim, Phys. Rev. **75**, 1716 (1949).
[20] I. E. Tamm and S. Belenky, J. Phys. U.S.S.R. **1**, 177 (1939).
[21] R. R. Wilson, Phys. Rev. **86**, 261 (1952).
[22] W. W. Brown, A. S. McKay, and E. D. Palmatier, Phys. Rev. **76**, 506 (1949).

about 0.8 for a 100-Mev shower and is only down to 0.6 for a 50-Mev shower.

The contribution to the corrected number of Type I events by knock-on showers can be estimated by calculating the part of Y_{k0} which is due to electrons of energy lower than E_s. To see how sensitive this correction is to the particular value of E_s chosen, the calculation was repeated for several different values. These calculations are similar to the one given above for Y_{k0}. The results are shown in Table II. The value of the expected number of detected events due to concealed knock-on showers is not very sensitive to the value chosen for E_s. The magnitude of the correction depends, however, as did Y_{k0} (total) on the accuracy of the photon track length formula at the giant resonance energy.

An upper limit on the correction can be obtained by assuming that all of the 109 ± 23 (ABC:N) Type II and III events (Table I) are due to knock-on showers (actually the observed positive:negative ratio of 1.8 ± 0.4 in this group contrasted with the value 1.25 for sea level μ mesons indicates a protonic admixture of about $20_{-20}^{+100}\%$ of the events) and that E_s is about 100 Mev. Then the number of Type I (ABC:N) events due to knock-on showers is

$$4.04\times10^{-4}\times109/(8.04\times10^{-4}-4.04\times10^{-4})=111.$$

This figure, since it involves the ratio of two track length calculations, is less sensitive to error in the track length formula used.

We take 100 ± 20 as the best estimate of the number of Type I ABC:N events due to neutrons from real photons absorbed from small knock-on showers. This corresponds to a yield of $(3.96\pm0.79)\times10^{-4}$ neutrons per μ meson per cm Pb, or a cross section-multiplicity product of $(5.8\pm1.2)\times10^{-29}$ cm^2 per nucleon.

To correct the momentum histogram of Fig. 4, we need to calculate the momentum spectrum of μ mesons producing knock-on showers detected by their neutron production. We need only stop our calculation before the final integration over P_μ, the μ-meson momentum, of dY_{k0}/dP_μ. To obtain the area under the spectrum we multiply this differential neutron yield by ABC rate $\times$running time$\times F\times F'\times\epsilon$, where F and F' have been defined in Sec. IV and ϵ is the coherent neutron detecting efficiency, 9.3%. For Type I ABC:N events we count only showers initiated by electrons of less than (100 ± 20) Mev energy. With this choice of E_s, the area comes out to be 63 ± 13 events. In the histograms of Fig. 5, this calculated knock-on shower spectrum has been substracted off, the three graphs A, B, and C corresponding to $E_s=100$, 80, and 120 Mev, respectively. The shape of the correction spectrum is much less in doubt than its height. The momentum distribution of μ mesons causing neutron production by means of knock-on showers should not be affected by the uncertainty in the formula for the low-energy photon track length, which, if wrong, should be in error in the same direction for all size showers. The shape is determined by relatively well-known quantities: the incident μ-meson spectrum, the knock-on probability, and the functional dependence of the low-energy photon track length on the initial shower energy.

TABLE II. Neutron yield, Y_{k0}, and expected number detected, N_{k0}, from knock-on showers of energy less than E_s.

E_s (Mev)	Y_{k0}	N_{k0}
75	$3.68\times10^{-4}z$	93
100	$4.04\times10^{-4}z$	102
150	$4.85\times10^{-4}z$	122
200	$5.38\times10^{-4}z$	136

VI. COMPARISON OF RESULTS WITH THEORY

(a) Number of Interactions

On the basis of the correction estimated in Sec. V, the number of direct μ-meson interactions with Pb in which no additional charged particle emerges from a $\frac{1}{2}$ inch thickness is $(262\pm25)-(100\pm20)=162\pm32$. This corresponds to $(6.4\pm1.6)\times10^{-4}$ neutron per μ meson per cm Pb, or $\sigma\bar{n}=(9.4\pm2.4)\times10^{-29}$ cm^2 per nucleon. Here the error has been increased to allow for the 10% uncertainty in the absolute neutron detecting efficiency. We now compare this result with theoretical expectations.

The only known mechanism for producing the observed effect is the direct Coulomb interaction between the μ meson and the nucleus. The effect has been calculated by the Williams-Weizsäcker approximation, in which use is made of the related cross sections for photonuclear transitions. These cross sections are known experimentally and are, indeed, the same as those used above in the calculation of Y_{k0}. The approximation is based on the strong resemblance between the almost completely transverse electric field of a relativistic particle and the purely transverse one of a photon, and proceeds by making a Fourier expansion of the particle field into an equivalent spectrum of virtual photons. An interaction is then assumed to proceed by the absorption of one of these virtual photons by the struck nucleus. The approximation requires that the incident particle be relativistic, $[1/(1-\beta^2)^{\frac{1}{2}}\gg1]$ and that the momentum transfer be transverse to the direction of the particle, which also must not be deflected appreciably by the collision. These conditions are all very well met for the low-energy transfer interactions studied in this experiment. The hodoscope should have eliminated interactions with large momentum transfer, as they would give rise to particle multiplicity.

The photon spectrum is given by

$$N(E_\gamma)dE_\gamma=\frac{2}{137\pi}\left[\ln\frac{E_\mu}{E_\gamma}-\ln\frac{mcb_{\min}}{\hbar}-\ln1.48\right]\frac{dE_\gamma}{E_\gamma}$$

TABLE III. Results of the Williams-Weizsäcker calculations of the nuclear interactions of the virtual photons. The numbers entered are Y_μ/z, the number of interactions per μ meson per cm Pb, and N_μ, the corresponding number of detected events expected in the present sample. The rows correspond to different more or less plausible choices of $b_{\min}$ in the Williams-Weizsäcker spectrum. The columns correspond to various upper limits of the energy transfer. The second and third column correspond roughly to type I events.

	All virtual photon energies (up to E_μ)		Virtual photon energies <500 Mev		Virtual photon energies <320 Mev	
	Y_μ/z	N_μ	Y_μ/z	N_μ	Y_μ/z	N_μ
$b_{\min}=(8.0/3.8)\times10^{-13}$ cm for grant resonance, $(0.8/3.8)\times10^{-13}$ cm at higher energies	12.97×10^{-4}	327	8.36×10^{-4}	211	6.77×10^{-4}	171
$b_{\min}=8.0\times10^{-13}$ cm for grant resonance, 0.8×10^{-13} cm at higher energies	8.26×10^{-4}	208	5.92×10^{-4}	149	4.86×10^{-4}	123
$b_{\min}=\hbar/m_\mu c$	6.46×10^{-4}	163	5.53×10^{-4}	139	4.84×10^{-4}	122

where $b_{\min}$ is the least impact parameter for the process considered. There seems to be considerable doubt over just what length to use for $b_{\min}$. Kessler and Kessler[23] use $b_{\min}=hc/k$ (where k/c is the transverse momentum transfer) in the case of very large energy transfers and very high μ-meson energy. Annis and Wilkins,[2] on the other hand, use $b_{\min}=\hbar/m_\mu c$ following an uncertainty principle argument by Heitler.[24] According to Dalitz and Yennie,[25] neither of these are in general correct. The least impact parameter $b_{\min}$ is rather to be taken as the larger of $hc/k_{\max}$ where $k_{\max}/c$ is the largest transverse momentum transfer strongly effective, and a quantity we shall call d, which is the radius of the region over which the interaction is strong. The latter, for the absorption of virtual photons through the giant resonance portion of the photonuclear cross section, should be related to the radius of the lead nucleus, for the giant resonance involves the nucleus as a whole. For absorption around the photon-pi-meson production peak, one should, rather, use the radius of an individual nucleon. The length $hc/k_{\max}$ is smaller than either of these, since $k_{\max}$ corresponds to a quite high energy.

Following a suggestion by Dalitz[26] we shall take for $b_{\min}$ around the giant resonance photon energy the value $R_{\mathrm{Pb}}/3.8$ where R_{Pb} is the radius of the lead nucleus, and for all higher energies $b_{\min}$ is taken to be $R_p/3.8$ where R_p is the nucleon radius. The factor 1/3.8 corresponds to the first root of $J_0(kR)$, which occurs at $kR=3.8$. The values used for the radii are 8.0×10^{-13} cm and 0.8×10^{-13} cm, respectively.

The calculation of the neutron yield from the "virtual photons" of the Williams-Weizsäcker spectrum is similar to that outlined in the preceding section for the neutron yield from real photons in knock-on showers, with the W–W spectrum replacing the integral of the differential photon track length over the knock-on electron spectrum. The same expressions have been used for the product of the photon cross section and neutron multiplicity and for the μ-meson spectrum. The results are shown in Table III. In each place in the table two numbers are entered. The first (left) is Y_μ/z, the neutron yield per μ meson per cm Pb. The second is the corresponding number of detected events expected in this experiment. The three rows give the results for three more or less plausible choices of $b_{\min}$—the first is that of Dalitz, the second that of Dalitz without the factor 3.8^{-1}, the third that of Heitler. The first column gives the results for the case where the integration is extended over all virtual photon energies, e.g., from 0 to E_μ, the μ-meson energy. Interactions of high-energy virtual photons will, however, make visible showers in the hodoscope; and for comparison with observed Type I $ABC{:}N$ events a high-energy cutoff on E_γ must be imposed. The second and third columns give the results when the cutoff is made at 500 and 320 Mev, respectively. These seem to be reasonable values. The interaction involves creation of one or more π mesons having most of the photon energy. If a π meson escapes from the nucleus it will almost certainly make a detected shower. Reabsorption of the π meson in the nucleus in which it is made will make stars that are expected to contain at least one penetrating prong (penetration of 1.27 cm Pb requires a minimum kinetic energy of 40 Mev for a π meson and 90 Mev for a proton).

In view of the uncertainties of $b_{\min}$ and the upper limit of E_s, we can only conclude that the expected number of directly produced Type I $ABC{:}N$ events is in the range 120 to 210. This result is to be compared with the experimental figure of 162 ± 32. Within the errors of the theoretical and experimental analyses, there is excellent agreement.

(b) Momentum Spectrum of Interacting μ Mesons

We can also compare the momentum spectrum of interacting μ mesons (Fig. 5) with that expected on the basis of the Williams-Weizsäcker calculation. In fact, some of the uncertainties cancel out when we consider spectral shape rather than absolute value. The calculated spectrum is obtained by stopping the calculation before integrating over P_μ, so obtaining the neutron yield per unit μ-meson momentum interval. The result obtained with E_γ cut off at 500 Mev is shown as the smooth curve in Fig. 5(a), (b), and (c) adjusted in height in each case to match the area of

[23] P. Kessler and D. Kessler, Compt. rend. **244**, 1896 (1957).
[24] W. Heitler, *The Quantum Theory of Radiation* (Oxford University Press, London, 1954), third edition, pp. 414–417.
[25] R. H. Dalitz and D. R. Yennie, Phys. Rev. **105**, 1598 (1957).
[26] R. H. Dalitz (private communication).

the histogram. The agreement between calculation and experiment is as good as can be expected. In Fig. 5(c) the fit is not as good as in Figs. 5(b) and 5(a), suggesting that E_s is more likely to be below than above 100 Mev.

(c) Variation of Neutron Yield with μ Meson Momentum

As has already been indicated in Sec. IV, comparison of the spectrum of interacting μ mesons with that of the incident μ mesons gives information on the variation of the neutron yield with μ-meson momentum. The experimental results are shown in the first row of Table IV. The Williams-Weizsäcker calculation can also be used to predict this variation; in fact, this is just another way of looking at the spectrum calculation just discussed. A logarithmic rise in $\sigma\bar{m}$ with P_μ is expected. The results are shown in the second row of Table IV. There is seen to be reasonable agreement, in view of the experimental and theoretical uncertainties.

TABLE IV. Change of neutron yield with μ-meson momentum. The number entered is the ratio, normalized to 1 in the first momentum interval, of the number of detected direct nuclear interactions [Fig. 5(a)] to the number of incident μ mesons in the same momentum interval.

	0.65–3 Bev/c	3–10 Bev/c	10 Bev/c
Observed [Fig. 5(a)]	1.0±0.25	1.8±0.3	3.2±1.0
Calculated as in first row, second column of Table III	1.0	1.9	4.5

VII. CONCLUSIONS

We have been able to determine the rate of μ-meson nuclear interactions in which the energy transfer to the nucleus is so small that no charged secondary particle emerges up or down from a 1.27 cm Pb plate, but at least one evaporation neutron emerges. The rate corresponds to a cross section-neutron multiplicity product of $(9.4\pm2.4)\times10^{-29}$ cm^2 per nucleon. This value is in the range of values predicted under various plausible forms of the Williams-Weizsäcker approximation method. Any further improvement in the experimental precision would be useless without a more rigorous calculation of the result expected from the electronuclear interaction; at present, theory is more uncertain than experiment.

The increase of neutron yield with μ-meson momentum is also in agreement with rough theoretical expectations.

We conclude that the observed effects can be ascribed to the electric charge of the μ-meson interacting with the nucleons of the target material. In terms of the Weizsäcker-Williams approximation, the effect is due to "virtual photons." If any other interaction is effective, its contribution cannot be greater in order of magnitude than the electronuclear one.

We have calculated the neutron yield from real photons in cascade showers initiated by knock-on electrons, finding 11.8×10^{-29} cm^2 per nucleon in lead. We have shown from the hodoscope observations in the ABC run that about half of the neutron producing showers are concealed in 1.27 cm Pb. It follows that most of the 99±15 visible shower $ABC{:}N$ events are due to knock-on electrons of μ mesons.

Previous experiments at this laboratory were unable to separate the direct and knock-on effects, and only gave the sum. The result of Stearns et al.,[2] $\sigma\bar{m}=(22\pm8)\times10^{-29}$ cm^2 per nucleon, is confirmed by our sum, $(21\pm2.7)\times10^{-29}$ cm^2 per nucleon. Their theoretical estimates of the expected direct and knock-on effects are also in good agreement with ours. The underground experiment of Wilkins,[2] carried out at a depth of 20 m water-equivalent, gave a total $\sigma\bar{m}$ of $(40\pm2)\times10^{-29}$ cm^2 per nucleon in Pb. At that depth the average μ-meson momentum is about 9 Bev/c, compared with 5 Bev/c in our experiment. In view of Table IV, the result seems reasonable. An explicit calculation for this depth of the underground μ-meson spectrum and the resulting real and virtual photon effects has not been made.

It was not possible to separate the direct interactions with large energy transfer from knock-on showers or high-energy proton events. Thus, no conclusions can be drawn about the behavior of the photonuclear cross section at high photon energies.

VIII. ACKNOWLEDGMENTS

We are grateful to J. D. Miller for his share in the construction, installation, and maintenance of the equipment; to J. E. Rizzo, Jr., for determining the optical distortions, to G. O. Monnig for calibrating the neutron source; and to J. D. Fox for completing the prism compensator and making many of the curvature measurements.

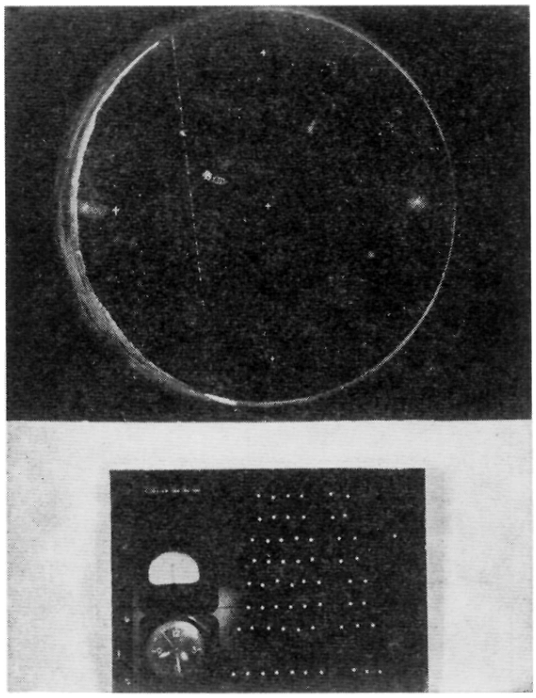

FIG. 2. Sample cloud chamber and hodoscope picture. The cloud chamber picture shows a single positively charged particle of 15 *Bev/c momentum. The hodoscope picture shows that it* penetrated the target hodoscope without any extra Geiger tubes being discharged and without appreciable scattering (the neon lights are not positioned exactly to scale).